

Multiple common envelope events from successive planetary companions

Luke Chamandy,¹★ Eric G. Blackman,¹† Jason Nordhaus^{2,3}‡ and Emily Wilson²§

¹*Department of Physics and Astronomy, University of Rochester, Rochester NY 14627, USA*

²*Center for Computational Relativity and Gravitation, Rochester Institute of Technology, Rochester, NY 14623, USA*

³*National Technical Institute for the Deaf, Rochester Institute of Technology, Rochester, NY 14623, USA*

22nd December 2024

ABSTRACT

Many stars harbour multi-planet systems. As these stars expand late in their evolution, the innermost planet may be engulfed, leading to a common envelope (CE) event. Even if this CE interaction is insufficient to eject the envelope, it may cause the star to expand further, leading to additional CE events, with the last one unbinding what remains of the envelope. This multi-planet CE scenario may have broad implications for stellar and planetary evolution across a range of systems. We develop a simplified version and show that it may be able to explain the recently observed planet WD 1856 b.

Key words: planetary systems: formation – white dwarfs – stars: AGB and post-AGB – binaries: close – stars: winds, outflows – accretion, accretion disks

1 INTRODUCTION

Vanderburg et al. (2020) (hereafter V20) recently detected the planet WD 1856 b orbiting a white dwarf (WD) with orbital period 1.4 d. It is well within the envelope of the progenitor star and inside of the WD-planet period gap predicted by Nordhaus et al. (2010), suggesting that a single common envelope (CE) origin is unlikely (Nordhaus & Spiegel 2013). V20 also argued against a single CE origin. Lagos et al. (2020) argued that a single CE event origin is possible, but requires special parameter values and energy input additional to the released orbital energy.

Based on a suite of detailed stellar interior models which match the initial-final mass relation (Cummins et al. 2018), we have also verified that the envelope of a star containing a WD core of mass $0.518 \pm 0.055 M_{\odot}$ can be ejected by a companion of $13.8 M_{\text{J}}$ only if the initial primary mass is $< 1.2 M_{\odot}$. In addition, assuming that orbital energy alone is used to eject the envelope with maximum efficiency (i.e. $\alpha_{\text{CE}} = 1.0$; Wilson & Nordhaus 2019, 2020), we checked that only a small handful of systems can unbind the envelope and emerge with the observed period. Successful single CE scenarios can only occur at late times with $< 0.1 M_{\odot}$ left in the envelope, and the average envelope-mass-to-core-mass ratio is < 0.14 .

Here we consider a new scenario that involves multiple CE events in succession, each involving a planet. Such a scenario was mentioned by Nordhaus et al. (2010), and recently by Lagos et al. (2020), but has not yet been quantitatively explored or studied in any specific context. We show that this scenario may explain WD 1856 b.

Possible pathways initiating CE have been previously discussed (e.g. Villaver & Livio 2009; Chen et al. 2018). Those may apply to the first CE interaction involving planet 1, but in the present context, a rapid expansion of the primary subsequently engulfs planet 2. We

restrict to cases where these two successive CE interactions, CE1 and CE2, combine to remove the envelope. We assume that planet 1 is disrupted in CE1 but that planet 2 survives in orbit after CE2.

In Sec. 2, we compute the respective fractions of the initial envelope binding energy injected during CE2 and CE1 for a given mass m_2 of planet 2. We then determine the mass m_1 of planet 1, exploring two limiting cases to bracket its range. For plausible models, CE1 should cause CE2. We estimate the expansion of the star during CE1, and show that it can be large enough for the star to engulf another, more distant planet. In Sec. 3, we refine this part of the model to account for radiative cooling.

2 TWO-PLANET COMMON ENVELOPE SCENARIO

2.1 Planet mass combinations for two limiting cases

To exemplify the model, we adopt the WD mass, radius, and planet 2 orbital radius used in V20: $M_{\text{wd}} = 0.518 M_{\odot}$, $R_{\text{wd}} = 1.31 \times 10^{-3} R_{\odot}$, and $P_2 = 1.408$ d. Subscript ‘1’ will delineate the state of the system at the start of CE1 and subscript ‘2’ at the start of CE2. We assume the mass of each planet to be constant, but allow for tidal disruption of planet 1. The binding energy (defined > 0) of the envelope at the start of mass transfer that leads to CE1 is given by

$$E_1 = \frac{GM_1 M_{e,1}}{\lambda_1 R_1}, \quad (1)$$

where G is the gravitational constant, M_1 is the original mass of the primary, $M_{e,1}$ is the original envelope mass, R_1 is the original radius of the primary and λ_1 is a conventional dimensionless parameter accounting for distinct energy profiles in radius. If a fraction β_1 of the energy needed to unbind the envelope is supplied by CE1, then CE2 need supply only a fraction $\beta_2 = 1 - \beta_1$ to unbind the remaining envelope. The CE energy formalism (e.g. Ivanova et al. 2013) applied

★ lchamandy@pas.rochester.edu

† blackman@pas.rochester.edu

‡ nordhaus@astro.rit.edu

§ ecw7497@rit.edu

to CE1 then gives

$$\beta_1 E_1 = (1 - \beta_2) E_1 \approx \alpha_1 \frac{GM_{\text{wd}} m_1}{2a_{f,1}}, \quad (2)$$

where α_1 is a conventional dimensionless parameter accounting for the energy conversion efficiency of the unbinding process, m_1 is the mass of planet 1, the primary core mass is assumed equal to M_{wd} , $a_{f,1}$ is the binary separation at the end of CE1, the small mass of the envelope interior to the orbit has been neglected (or can be absorbed into the factor β_1), and the term $-\alpha_1 GM_1 m_1 / 2a_{i,1}$ on the right side (with $a_{i,1}$ the initial separation) is neglected as in V20; we have checked that this term is generally small. For CE2 with similar assumptions, we have

$$\beta_2 E_1 \approx \alpha_2 \frac{GM_{\text{wd}} m_2}{2a_{f,2}}. \quad (3)$$

Dividing equation (2) by equation (3), and rearranging, we obtain

$$m_1 = \frac{a_{f,1}}{a_{f,2}} \frac{\alpha_2}{\alpha_1} \left(\frac{1}{\beta_2} - 1 \right) m_2. \quad (4)$$

The quantity m_2 is not known precisely but was constrained by V20 to have an upper limit of about $14 M_{\text{J}}$. Next, we divide equation (3) by equation (1) to obtain

$$\beta_2 = \frac{M_{\text{wd}} m_2}{2(M_1 - M_{\text{wd}}) M_1} \frac{\alpha_1 \lambda_1 R_1}{a_{f,2}} \frac{\alpha_2}{\alpha_1}, \quad (5)$$

where we have substituted $M_{e,1} = M_1 - M_{\text{wd}}$. The quantity $a_{f,2}$ is related to the observed period by Kepler's third law:

$$a_{f,2} = \left[G(M_{\text{wd}} + m_2) \left(\frac{P_{f,2}}{2\pi} \right)^2 \right]^{1/3} \approx \left(\frac{GM_{\text{wd}} P_{f,2}^2}{4\pi^2} \right)^{1/3}, \quad (6)$$

where $P_{f,2} = 1.4$ d is the observed period (in the rightmost expression and below we neglect the mass of either planet compared to the WD).

In the top panel of Fig. 1 we plot β_2 against m_2 , in Jupiter masses, for various values of $\alpha_1 \lambda_1$ chosen to be consistent with estimates of V20, for either $M_1 = 1 M_{\odot}$ or $M_1 = 3 M_{\odot}$. Since $\beta_2 < 1$ for $m_2 < 14 M_{\text{J}}$, a single CE scenario fails, in agreement with V20. On the other hand, extremely small values of β_2 would require fine-tuning β_1 to be just less than 1. We see that β_2 can take on values up to 0.15 for $m_2 < 14 M_{\odot}$. Focusing on $\beta_2 > 0.01$ gives $\alpha_1 \lambda_1 \gtrsim 0.4$ in the $3 M_{\odot}$ model and also determines a corresponding lower limit on m_2 .

Following V20, we assume R_1 to be equal to the primary's Roche lobe when mass transfer initiates, and then make use of their fitting formula for R_1 in terms of M_{wd} . This gives

$$R_1 = 5.56 \times 10^4 f(M_{\text{wd}}/M_{\odot}) R_{\odot}, \quad (7)$$

where

$$f(\mu) \equiv \frac{\mu^{19/3}}{1 + 20\mu^3 + 10\mu^6} + f_0,$$

with $f_0 = 7.2 \times 10^{-5}$.

For $a_{f,1}$, we consider two limiting cases: (i) the planet merges with the WD, with all of the liberated orbital energy released to the envelope so

$$a_{f,1} \approx R_{\text{wd}} \approx 1.3 \times 10^{-3} R_{\odot} \quad (\text{case i}), \quad (8)$$

and (ii) after the planet gets tidally disrupted, its orbital energy is no longer used to unbind the envelope. In this case, we can estimate (c.f.

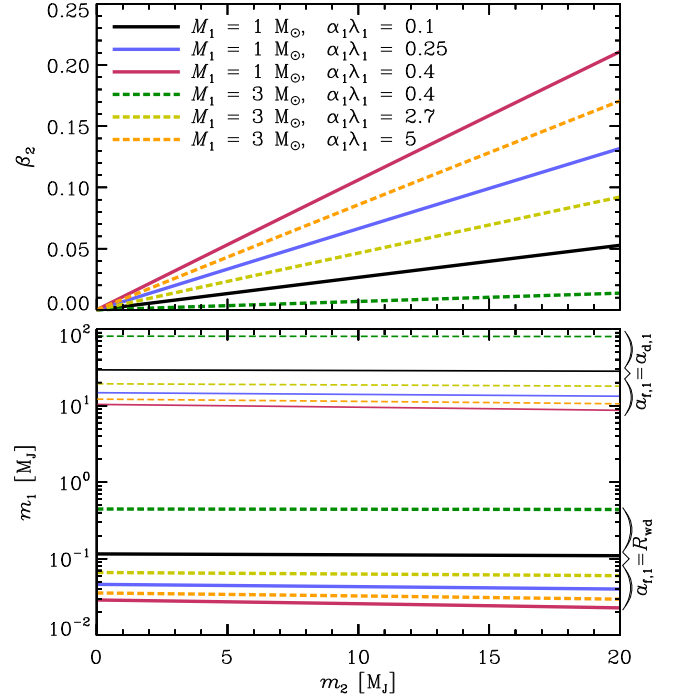


Figure 1. *Top:* The fraction β_2 of the original binding energy E_1 injected during CE2. *Bottom:* The mass m_1 of planet 1 required to inject the fraction $\beta_1 = 1 - \beta_2$ of the binding energy E_1 , assuming that the final separation is equal to the WD radius, $a_{f,1} = R_{\text{wd}}$ (thick lines), or to the tidal disruption separation, $a_{f,1} = a_{d,1}$ (thin lines). The latter is calculated under the assumption that the planet radius $r_1 = 0.1 R_{\odot}$. In both panels $\alpha_1/\alpha_2 = 1$ is used.

Nordhaus & Blackman 2006)

$$\begin{aligned} a_{f,1} &= a_{d,1} \approx \left(\frac{2M_{\text{wd}}}{m_1} \right)^{1/3} r_1 \quad (\text{case ii}) \\ &\approx 0.2 R_{\odot} \left(\frac{M_{\text{wd}}}{0.52 M_{\odot}} \right)^{1/3} \left(\frac{m_1}{10^{-4} M_{\odot}} \right)^{-1/3} \left(\frac{r_1}{10^{-2} R_{\odot}} \right), \end{aligned} \quad (9)$$

where $a_{d,1}$ is the tidal disruption radius, measured from the centre of the primary's core, and r_1 is the radius of planet 1. Cases (i) and (ii) bracket the range of possibilities.

Equation (4), with equations (5), (6), (7), and (8) or (9), are then used to obtain m_1 in terms of $\alpha_1 \lambda_1$, $a_{f,1}$, m_2 , $P_{f,2}$, M_{wd} , M_1 and the ratio α_2/α_1 . The results are plotted in the bottom panel of Fig. 1, for $\alpha_1/\alpha_2 = 1$ and the parameter values mentioned in the figure legend and caption. Case (i), $a_{f,1} = R_{\text{wd}}$, is represented by thick lines, and thin lines show case (ii), $a_{f,1} = a_{d,1}$, assuming $r_1 = 0.1 R_{\odot}$. For $M_1 = 1 M_{\odot}$, we see that the required planet mass needed to inject the fraction β_1 of the original envelope binding energy falls within the reasonable range of $0.02 \lesssim M_1/M_{\text{J}} \lesssim 30$. For $M_1 = 3 M_{\odot}$ we obtain $0.03 \lesssim M_1/M_{\text{J}} \lesssim 0.5$ if $a_{f,1} = R_{\text{wd}}$, but $10 \lesssim M_1/M_{\text{J}} \lesssim 80$ if $a_{f,1} = a_{d,1}$ is adopted. The latter range falls mostly above the usual planet-brown dwarf boundary of $\sim 13 M_{\odot}$.

Fig. 1 shows that there is a large section of parameter space that produces $\beta_2 > 0.01$ and realistic values for m_1 . The smaller value of $M_1 = 1 M_{\odot}$ (solid lines) leads to a larger viable parameter space than with $M_1 = 3 M_{\odot}$ (dashed lines). The $1 M_{\odot}$ value may also be favoured simply because the initial mass function is weighted toward lower-mass progenitors (Chabrier 2003).

2.2 Expansion of the envelope during CE1

While it is possible that the primary star could expand on its canonical evolutionary time (\gtrsim Myr) to eventually engulf planet 2, this time is much longer than typical CE plunge times of days to years. Here we explain why planet 2 could be engulfed, simply as a *result* of CE1.

During CE1, energy is predominantly deposited into the envelope near its base, due to the $1/r$ potential and centrally condensed structure of the evolved star. We expect the envelope to dynamically respond by expanding. To estimate the expansion, we equate the initial energy just after CE1 with the final energy after the envelope has adjusted. While the envelope might incur oscillations (Clayton et al. 2017), we are interested in the maximum radius reached, so neglecting this possibility implies that our model is conservative. Likewise, we neglect the possible release of recombination energy as the envelope expands, also a conservative choice. We do not include a bulk kinetic energy term for the bound envelope but do allow for the possibility that escaping winds are launched. We obtain

$$-(1 - \beta_1) \frac{GM_1 M_{e,1}}{\lambda_1 R_1} = -\frac{GM_2 M_{e,2}}{\lambda_2 R_2} + E_{ej}. \quad (10)$$

where E_{ej} is the energy of the ejecta (wind), which is not well constrained. If the ejecta leaves at the escape speed, it will remove only a net thermal energy because bulk kinetic and potential energies sum to zero in this case. For convenience, we write

$$E_{ej} = \frac{1}{2} C' \frac{M_{ej} v_{esc,2}^2}{\lambda_2} = \frac{C' GM_2 (M_{e,1} - M_{e,2})}{\lambda_2 R_2}, \quad (11)$$

with $M_{ej} = M_{e,1} - M_{e,2}$ the ejecta mass, $v_{esc,2}$ the escape speed from the surface of the star in its final state, and C' a dimensionless constant. Substituting equation (11) into equation (10), and defining $\lambda'_2 \equiv \lambda_2 M_{e,2} / (M_{e,2} - C' M_{ej})$, the right side of equation (10) becomes $-GM_2 M_{e,2} / \lambda'_2 R_2$. Note that $\lambda'_2 \rightarrow \lambda_2$ as $C' \rightarrow 0$ or $E_{ej} \rightarrow 0$. Further, equation (10) can be rearranged to give

$$\frac{R_2}{R_1} = \frac{1}{\beta_2} \frac{\lambda_1}{\lambda'_2} \frac{M_2}{M_1} \frac{M_{e,2}}{M_{e,1}}. \quad (12)$$

The mass of the ejecta M_{ej} cannot exceed $M_{e,1} / (1 + C')$ or else R_2 reduces to zero; we focus on solutions for which $R_2 > R_1$, which requires M_{ej} to be less than some smaller critical value. If $M_{ej} = 0$, then $M_{e,2} = M_{e,1}$ and the solution reduces to

$$\frac{R_2}{R_1} = \frac{1}{\beta_2} \frac{\lambda_1}{\lambda_2}; \quad (\text{no mass loss}). \quad (13)$$

As example I, we take $M_1 = 1 M_\odot$ so that $M_{e,1} = M_1 - M_{wd} \approx 0.48 M_\odot$, and adopt $\lambda_1 = \lambda_2$, $C' = 1$, and $\beta_2 = 0.1$. Then, in the limit of no mass loss we obtain $R_2 = 10R_1$. The maximum ejecta mass ($R_2 = 0$) is $\approx 0.24 M_\odot$, whilst $R_2 = R_1$ for $M_{ej} \approx 0.21 M_\odot$. If $M_{ej} = 0.1 M_\odot$, we obtain $R_2 = 5.3R_1$. As example II, we take $M_1 = 3 M_\odot$, which gives $M_{e,1} \approx 2.48 M_\odot$, and also choose $\lambda_2 = 3\lambda_1$ (c.f. Xu & Li 2010), $C' = 3$, and $M_{ej} = 0.3 M_\odot$. Then we obtain $R_2 = 1.5R_1$. For $M_{ej} = 0$, we obtain $R_2 = 3.3R_1$. These examples show that we can easily find cases where the envelope expands enough to engulf a second planet.

3 ROLE OF COOLING

3.1 Expansion including cooling

Not all of the energy injected into the envelope during the CE phase contributes to unbinding it. This includes, but is not limited to, energy lost via radiation that would have otherwise assisted unbinding.

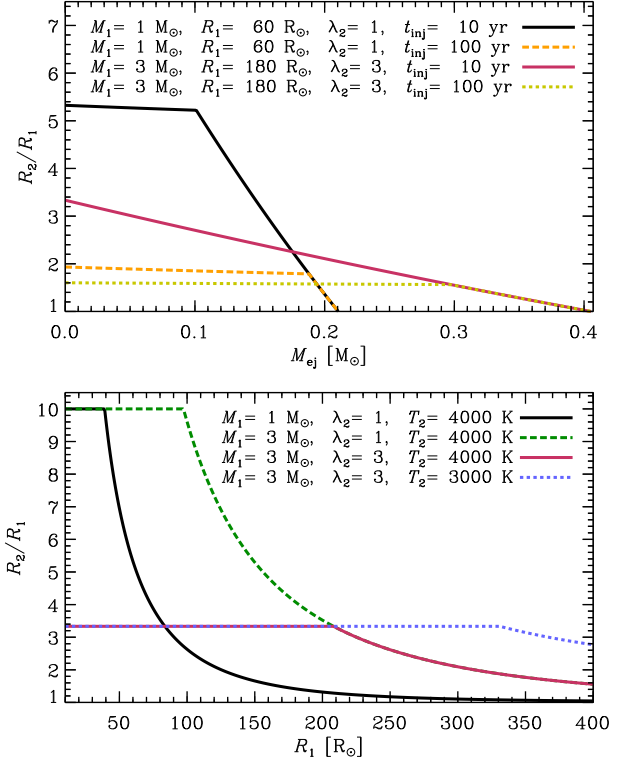


Figure 2. *Top:* The ratio R_2/R_1 of the stellar radius before and after CE1, as a function of the ejecta mass M_{ej} , with R_2 calculated from equation (14). The steeper part of each curve corresponds to $R_2 = R_{2,max}$, obtained when cooling is neglected, i.e. when $t_{thm} > t_{inj}$ in our model. If $t_{thm} = t_{inj}$, then $R_2 = R_{2,thm}$. All models have $\beta_1 = 0.9$, $\lambda_1 = 1$, $C' = \lambda_2$, and $T_1 = T_2 = 4 \times 10^3$ K. *Bottom:* The ratio R_2/R_1 plotted against the original radius R_1 , for the case $M_{ej} = 0$. All curves assume $\beta_1 = 0.9$, $\lambda_1 = 1$, $C' = \lambda_2$, $T_1 = 4 \times 10^3$ K, and $t_{inj} = 10$ yr. Wherever $t_{thm} > t_{inj}$, R_2/R_1 is independent of R_1 and the curve becomes flat.

This is among the inefficiencies included in the α -parameter of equations (2) and (3).

However, if cooling is as fast as energy injection, a “self-regulated” state could be reached with the energy injected swiftly radiated (Meyer & Meyer-Hofmeister 1979; Ivanova et al. 2013), and the expansion of CE1 quenched. Here we modify the calculation of Sec. 2.2 to account for this.

We postulate that with cooling, either the star expands until it reaches the radius calculated in Sec. 2.2 or until the energy loss and injection rates balance. Thus, we can write

$$R_2 = \min(R_{2,thm}, R_{2,max}), \quad (14)$$

where $R_{2,max}$ is the value of R_2 calculated in Sec. 2.2, and $R_{2,thm}$ is estimated by equating the mean rate of energy injection to the mean rate of energy loss due to radiative cooling and winds, namely

$$\beta_1 \frac{GM_1 M_{e,1}}{\lambda_1 R_1 t_{inj}} \sim 4\pi\sigma (R_{2,thm}^2 T_2^4 - R_1^2 T_1^4) + \frac{C' GM_2 M_{ej}}{\lambda_2 R_2 t_{inj}}, \quad (15)$$

where: t_{inj} is the time over which most of the energy is injected during CE1; the left side is equal to the rate of energy injection E_{inj}/t_{inj} ; the first term on the right side is the change in luminosity ΔL ; T_1 and T_2 are the effective temperatures of the star before and after CE1; and the last term is the rate of energy transfer to ejecta, E_{ej}/t_{inj} .

The transition from $R_2 = R_{2,\text{thm}}$ to $R_2 = R_{2,\text{max}}$ happens when t_{inj} becomes shorter than the radiative cooling time, given by

$$t_{\text{thm}} = \frac{E_{\text{inj}} - E_{\text{ej}}}{\Delta L}. \quad (16)$$

Equation (15) reduces to a cubic equation in $R_{2,\text{thm}}$,

$$R_{2,\text{thm}}^3 + bR_{2,\text{thm}} + c \sim 0, \quad (17)$$

where

$$b = - \left[\frac{\beta_1 A M_1 M_{\text{ej}}}{\lambda_1 R_1} + R_1^2 \left(\frac{T_1}{T_2} \right)^4 \right], \quad c = \frac{C' A M_2 M_{\text{ej}}}{\lambda_2},$$

with $A \equiv G/4\pi\sigma T_2^4 t_{\text{inj}}$. The relevant solution is

$$R_{2,\text{thm}} = 2\sqrt{-\frac{b}{3}} \cos \left[\frac{1}{3} \arccos \left(\frac{3c}{2b} \sqrt{-\frac{3}{b}} \right) \right]. \quad (18)$$

If $E_{\text{ej}} = 0$, then $c = 0$ and $R_{2,\text{thm}} = \sqrt{-b}$.

In the top panel of Fig. 2, we plot R_2/R_1 against M_{ej} for four different models. All models assume $\beta_1 = 0.9$, $\lambda_1 = 1$, and $C' = \lambda_2$. The solution can transition from $R_{2,\text{max}}/R_1$ (steeper portion of the curves) to $R_{2,\text{thm}}/R_1$ (flatter portion) when M_{ej} drops below some critical value. We consider our two example primary stars from Sec. 2.2. However, now the solution also depends on R_1 , which we set to $60 R_\odot$ ($180 R_\odot$) for the $1 M_\odot$ ($3 M_\odot$) star, and λ_2 , which we set to 1 (3), so that the ratio $\lambda_2/\lambda_1 = 1$ (3) is preserved from those examples. In addition, we illustrate two different values of t_{inj} : 10 yr and 100 yr; these choices are motivated in Sec. 3.2. Finally, we adopt $T_1 = T_2 = 4 \times 10^3$ K for each curve. We see that $R_2/R_1 \sim 1.5$ – 5 if $M_{\text{ej}} \lesssim 0.2 M_\odot$.

In the bottom panel, we adopt $M_{\text{ej}} = 0$, i.e. zero mass loss during CE1, as well as $t_{\text{inj}} = 10$ yr, and plot R_2/R_1 against R_1 , changing one parameter value at a time in each of the models plotted. The solution changes from $R_{2,\text{max}}/R_1$ (flat) to $R_{2,\text{thm}}/R_1$ at some critical value of R_1 . As in the top panel, all models assume $\beta_1 = 0.9$, $\lambda_1 = 1$, and $C' = \lambda_2$. Note that reducing T_2 causes a reduction in ΔL_{rad} , which can increase R_2/R_1 , so our choice of $T_2 = T_1$ for most of the curves is conservative. The black (red) curve in the top and bottom panels corresponds to the same overall model, sliced through $R_1 = 60 R_\odot$ ($R_1 = 180 R_\odot$) in the top panel and $M_{\text{ej}} = 0$ in the bottom.

3.2 Injection time scale

Here we estimate the time scale for energy injection into the envelope, t_{inj} , motivating the example values of Sec. 3.1. We consider the two limiting cases of Sec. 2.1. In case (i) the tidally disrupted planet is accreted onto the WD and most of the orbital energy is liberated after tidal disruption. This phase is still not well understood, but if an accretion disk sustains (Guidarelli et al. 2019), the pertinent Eddington accretion rate can be estimated as (e.g. Chamandy et al. 2018)

$$\dot{M}_{\text{Edd}} \sim 2 \times 10^{-3} M_\odot \text{ yr}^{-1} \left(\frac{R_{\text{wd}}}{1 R_\odot} \right), \quad (19)$$

with a corresponding accretion, and thus injection time

$$t_{\text{inj}} = t_{\text{acc}} \sim \frac{m_1}{\dot{M}} \sim 4 \times 10^1 \text{ yr} \left(\frac{m_1}{10^{-4} M_\odot} \right) \left(\frac{R_{\text{wd}}}{1.3 \times 10^{-3} R_\odot} \right)^{-1}. \quad (20)$$

On the other hand, dissipative forces during tidal disruption could redistribute angular momentum, leaving much low angular momentum

material to rapidly fall into the core (Guidarelli et al., in preparation). Overall, for case (i) we thus crudely estimate $1 \lesssim t_{\text{inj}} \lesssim 100$ yr.

For case (ii), where orbital energy is only released prior to tidal disruption, angular momentum transfer is dominated by hydrodynamic rather than dynamical friction deep inside the envelope (e.g. Chamandy et al. 2019), and we obtain t_{inj} to be much smaller than for case (i).

The envelope responds to energy injection on its sound-crossing time, which is of the order of days to months. If the energy is deposited at the base of the convective zone, then convection will transfer it to the envelope on a convective time, which is a few sound-crossing times. If energy is deposited in a deeper radiative zone, this further delays the energy to the envelope by a time scale of order the photon diffusion time, up to ~ 10 yr using the estimate in Chamandy et al. (2019). The envelope would continue to adjust dynamically as this energy is transferred. These processes might forestall the response of the envelope but are unlikely to change its duration. It is therefore reasonable to assume, as we have done in Sec. 3.1, that the envelope responds dynamically over the time $\sim t_{\text{inj}}$.

4 CONCLUSIONS

We explored a scenario whereby two planets undergo a CE event in succession, and the combined injection of energy from these events ultimately ejects the envelope.

Applied to the WD 1856 system, a planet whose orbit was interior to the initial orbit of WD 1856 b could have undergone a CE event (CE1) that resulted in the tidal disruption of the planet and partially unbound the envelope. This event would likely have caused the star to rapidly expand and engulf WD 1856 b, leading to a second CE event (CE2). CE2 would then have ejected the envelope with the planet orbit stabilized in its observed state. Setting aside the most conservative and most liberal extremes, $0.1 \lesssim m_1/M_J \lesssim 10$ emerges from our calculations as a plausible range for the mass of the planet involved in CE1.

We estimated the radius increase of the star during CE1 using energy arguments and allowing for mass loss and radiative cooling. For most of the plausible parameter space, we find the ratio of final to initial radii in the range $1.5 \lesssim R_2/R_1 \lesssim 10$. CE1 can thus plausibly lead to the engulfment of planet 2 and the initiation of CE2. However, the envelope cannot expand if the ejecta carries away too much energy. This might be mitigated if the drag on the secondary is substantial, but very fast moving ejecta will not have much time for drag.

Though we focused on a two-planet scenario, in general, more than two successive CE events with lower mass planets could contribute to envelope unbinding, with only the final event ejecting the envelope and hence avoiding disruption.

We expect the final planet left over after multiple CE events to be relatively massive, since massive planets are more likely to eject whatever remains of the envelope they enter. Thus, we might expect future detections of planets in close orbits around WDs to be skewed toward higher masses.

As our scenario involves previous mergers of planets with the stellar core, evidence of such mergers would be expected. One could search for chemical enrichment of the WD (e.g. Doyle et al. 2019), though old systems may no longer reveal this evidence if the planet material has long since accreted. Isolated high-field magnetic WDs are thought to have acquired their magnetic fields through accretion of a tidally disrupted companion, so the WDs in such systems might have higher-than-average magnetic fields (Nordhaus et al. 2011).

The notion that the envelope of the primary would expand significantly during a CE interaction with a planet is supported by findings of Staff et al. (2016), who simulated CE interactions between a 10 M_J planet and a 3.5 M_\odot RGB star or 3.05 M_\odot AGB star, and found that the envelope expands by $\sim 40\%$ or $\sim 20\%$, respectively. Higher resolution simulations that can follow the inspiral down to smaller separations, and thus greater release of orbital energy, would be very interesting.

References

- Chabrier G., 2003, *PASP*, **115**, 763
 Chamandy L., et al., 2018, *MNRAS*, **480**, 1898
 Chamandy L., Blackman E. G., Frank A., Carroll-Nellenback J., Zou Y., Tu Y., 2019, *MNRAS*, **490**, 3727
 Chen Z., Blackman E. G., Nordhaus J., Frank A., Carroll-Nellenback J., 2018, *MNRAS*, **473**, 747
 Clayton M., Podsiadlowski P., Ivanova N., Justham S., 2017, *MNRAS*, **470**, 1788
 Cummings J. D., Kalirai J. S., Tremblay P. E., Ramirez-Ruiz E., Choi J., 2018, *ApJ*, **866**, 21
 Doyle A. E., Young E. D., Klein B., Zuckerman B., Schlichting H. E., 2019, *Science*, **366**, 356
 Guidarelli G., Nordhaus J., Chamandy L., Chen Z., Blackman E. G., Frank A., Carroll-Nellenback J., Liu B., 2019, *MNRAS*, **490**, 1179
 Ivanova N., et al., 2013, *ARA&A*, **21**, 59
 Lagos F., Schreiber M. R., Zorotovic M., Gänsicke B. T., Ronco M. P., Hamers A. S., 2020, arXiv e-prints, p. [arXiv:2010.09747](https://arxiv.org/abs/2010.09747)
 Meyer F., Meyer-Hofmeister E., 1979, *A&A*, **78**, 167
 Nordhaus J., Blackman E. G., 2006, *MNRAS*, **370**, 2004
 Nordhaus J., Spiegel D. S., 2013, *MNRAS*, **432**, 500
 Nordhaus J., Spiegel D. S., Ibgui L., Goodman J., Burrows A., 2010, *MNRAS*, **408**, 631
 Nordhaus J., Wellons S., Spiegel D. S., Metzger B. D., Blackman E. G., 2011, *Proceedings of the National Academy of Science*, **108**, 3135
 Staff J. E., De Marco O., Wood P., Galaviz P., Passy J.-C., 2016, *MNRAS*, **458**, 832
 Vanderburg A., et al., 2020, *Nature*, **585**, 363
 Villaver E., Livio M., 2009, *ApJ*, **705**, L81
 Wilson E. C., Nordhaus J., 2019, *MNRAS*, **485**, 4492
 Wilson E. C., Nordhaus J., 2020, *MNRAS*, **497**, 1895
 Xu X.-J., Li X.-D., 2010, *ApJ*, **716**, 114

ACKNOWLEDGEMENTS

The authors thank Adam Frank for discussions. Financial support for this project was provided by the Department of Energy grant DE-SC0001063, DE-SC0020432 and DE-SC0020103, the National Science Foundation grants AST-1515648 and AST-1813298, PHY-2020249, and the Space Telescope Science Institute grant HST-AR-12832.01-A.